ARTICLES
https://doi.org/10.1038/s41551-018-0247-5

nature biomedical engineering

Sustained release of targeted cardiac therapy with a replenishable implanted epicardial reservoir

William Whyte[1,2,3,4,5,12], Ellen T. Roche[1,2,6,7,8,9,10,12], Claudia E. Varela[8,10], Keegan Mendez[1,2], Shahrin Islam[9], Hugh O'Neill[3], Fiona Weafer[6], Reyhaneh Neghabat Shirazi[6], James C. Weaver[1,2], Nikolay V. Vasilyev[11], Peter E. McHugh[6], Bruce Murphy[4,5], Garry P. Duffy[3,4,5,7,13*], Conor J. Walsh[1,2,13*] and David J. Mooney[1,2,13*]

The clinical translation of regenerative therapy for the diseased heart, whether in the form of cells, macromolecules or small molecules, is hampered by several factors: the poor retention and short biological half-life of the therapeutic agent, the adverse side effects from systemic delivery, and difficulties with the administration of multiple doses. Here, we report the development and application of a therapeutic epicardial device that enables sustained and repeated administration of small molecules, macromolecules and cells directly to the epicardium via a polymer-based reservoir connected to a subcutaneous port. In a myocardial infarct rodent model, we show that repeated administration of cells over a four-week period using the epicardial reservoir provided functional benefits in ejection fraction, fractional shortening and stroke work, compared to a single injection of cells and to no treatment. The pre-clinical use of the therapeutic epicardial reservoir as a research model may enable insights into regenerative cardiac therapy, and assist the development of experimental therapies towards clinical use.

Although technological advances in coronary artery revascularization therapies have proved to be successful at restoring blood flow to the heart after a myocardial infarction (MI) or heart attack, residual myocardial scarring often remains. Elimination of scarring and restoration of full cardiac function post-MI could eliminate or attenuate the cascade of events that lead to ischaemic heart failure. While effective clinical therapies in this domain are lacking, simple single deliveries of cells[1,2], growth factors[3–10] or drugs[11–16] has shown promise, especially pre-clinically. A common theme underpinning these studies is poor retention and survival at the diseased site, and the necessity for repeated or sustained delivery for best efficacy[17–19].

Stem cells, in particular, have attracted intense interest as a cardiac regenerative therapy, but so far only modest or inconsistent functional benefits have been reported in clinical trials[20]. Synthesis and secretion of paracrine factors is believed to be the main mechanism of action[21–24], and extending the viability of these transplanted cells within the harsh environment of the post-MI or chronic ischaemic heart is likely to be key to this effect. It is accepted that biomaterial delivery vehicles enhance cardiac cellular retention and survival in comparison to physiological saline, offering hope for future trials using this delivery vehicle[25–36]. Furthermore, recent evidence supports a paradigm shift towards repeated cell administration, demonstrating that multiple administrations are therapeutically superior to single doses in MI and heart failure animal models[37,38]. A method to replenish therapy, or offer multiple administrations without necessitating multiple surgeries, has not yet been demonstrated, motivating the design of this system.

Advanced delivery strategies have been identified as an important area of research and development to fully realize the promise of regenerative therapies[39,40]. Potential improvements include minimally invasive catheter delivery of therapy and the use of a biomaterial carrier vehicle that can be refilled[41], allowing for increased bioavailability of these agents at the pathological site within a suitable therapeutic window. Such an approach could be used for the delivery of (1) small bioactive molecules free-loaded into a biomaterial matrix, (2) proteins/macromolecules that could diffuse across a membrane in a controlled fashion, or (3) a cell payload facilitating release of bioactive molecules that exert therapeutic effects on local tissue for sustained periods. Here, we present an implantable system that can act as a vehicle for any of these approaches and allow for multiple replenishments of therapy without further surgery.

Results

Vision, design and realization of the Therepi system. Here we introduce 'Therepi', a therapeutic, epicardially placed reservoir that offers many advantageous features to address the current limitations for the delivery of small molecules, macromolecules and cells to treat cardiac disease. The vision for clinical translation is that a therapeutic reservoir is placed on the border zone of the infarcted

[1]John A. Paulson School of Engineering and Applied Sciences, Harvard University, Cambridge, MA, USA. [2]Wyss Institute for Biologically Inspired Engineering, Harvard University, Cambridge, MA, USA. [3]Tissue Engineering Research Group, Department of Anatomy, Royal College of Surgeons in Ireland, Dublin, Ireland. [4]Trinity Centre for Bioengineering, Trinity College Dublin, Dublin, Ireland. [5]Advanced Materials and BioEngineering Research (AMBER) Centre, Royal College of Surgeons in Ireland, National University of Ireland Galway and Trinity College Dublin, Dublin, Ireland. [6]Biomedical Engineering, College of Engineering and Informatics, National University of Ireland Galway, Ireland. [7]Department of Anatomy, School of Medicine, College of Medicine Nursing and Health Sciences, National University of Ireland Galway, Ireland. [8]Institute for Medical Engineering and Science, Massachusetts Institute of Technology, Cambridge, MA, USA. [9]Department of Mechanical Engineering, Massachusetts Institute of Technology, Cambridge, MA, USA. [10]Harvard-MIT Program in Health Sciences and Technology, Cambridge, MA, USA. [11]Department of Cardiac Surgery, Boston Children's Hospital, Boston, MA, USA. [12]These authors contributed equally to this work: William Whyte, Ellen T. Roche. [13]These authors jointly supervised this work: Garry P. Duffy, Conor J. Walsh, David J. Mooney. *e-mail: garry.duffy@nuigalway.ie; walsh@seas.harvard.edu; mooneyd@seas.harvard.edu

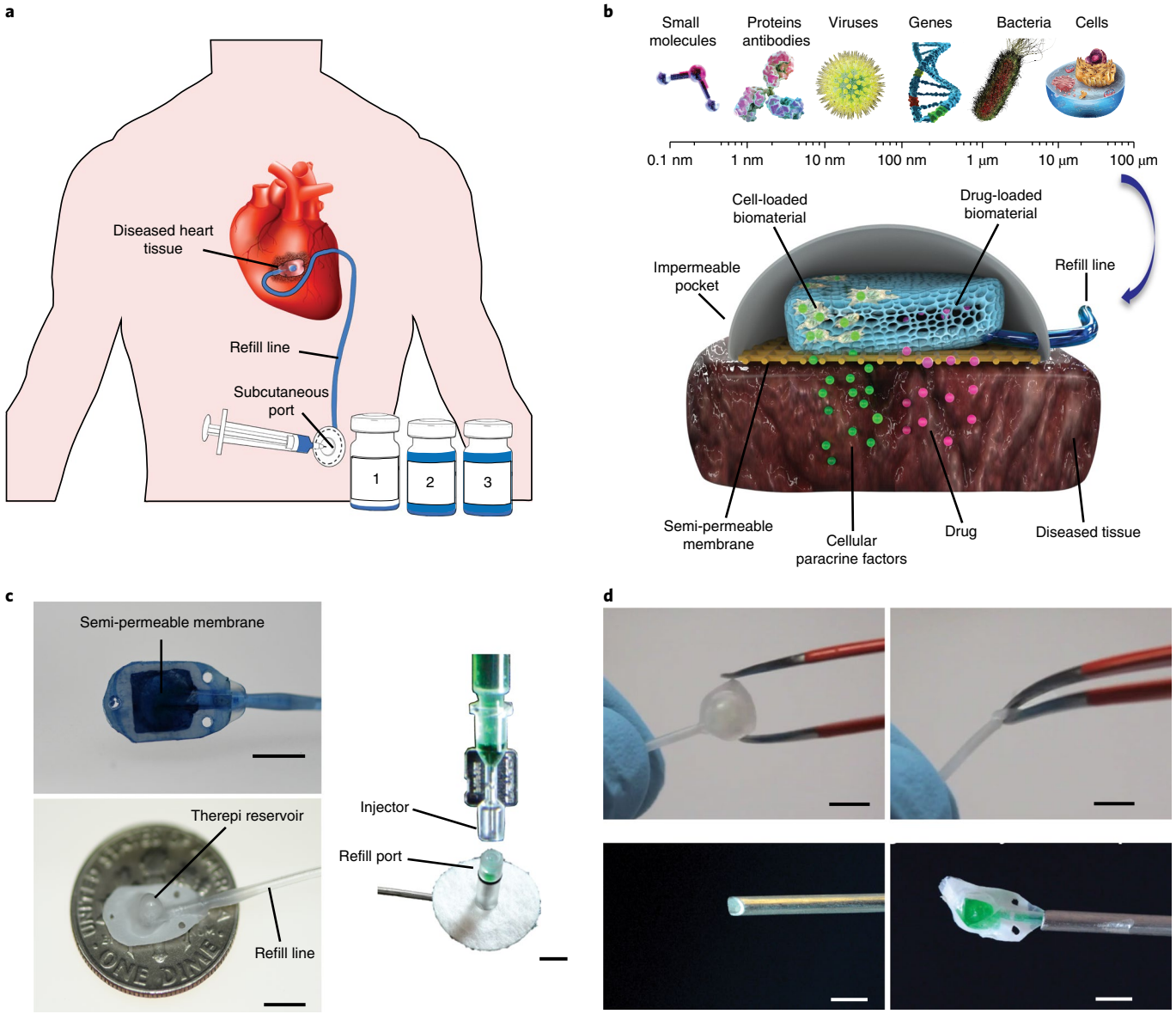

Fig. 1 | An overview of the vision for the clinical translation of Therepi and its realization for pre-clinical evaluation. a, Our vision for translation of the Therepi system to the clinic. The patient is injecting therapy through a subcutaneous port connected to a reservoir at the heart surface via a refill line. **b**, An overview of the Therepi system mechanism of action. Small molecules/macromolecules or paracrine factors from cells are released through the semi-permeable membrane. A refill line for targeted replenishment of therapy is shown on the far right. **c**, The pre-clinical realization of Therepi. Top left: a view of the Therepi reservoir from the tissue-contacting interface, dyed blue to aid visualization. Bottom left: the Therepi reservoir placed on a dime for size reference and connected to a self-sealing subcutaneous port. Right: the specialized injector for the self-sealing port. **d**, Top: compression and recovery of the Therepi with tweezers, showcasing flexibility. Bottom: the delivery of Therepi through a 14G needle. Scale bars, 4 mm.

heart and connected to a subcutaneous port or self-sealing rubber septum by an indwelling catheter, thus enabling multiple minimally invasive replenishments directly to the target site without the need for higher systemic doses (Fig. 1a).

The system offers a method to tune the rate of therapy diffusion and limit the size of molecules diffusing into tissue by varying the porosity of the semi-permeable membrane (Fig. 1b). We also incorporated a biomaterial vehicle into the system to promote retention of the delivered cargo and enhance engraftment and viability of cells. In this work, we used two model biomaterials: a methacrylated gelatin cryogel, GelMA[42], and Gelfoam, a commercially available gelatin sponge. However, we foresee this system working with a large panel of biomaterials, including, but not limited to, alginate[33], chitosan[31], hyaluronic-acid-based gels[26,36] and collagen[2,43].

Details of the design and manufacture of the Therepi system are described in the Supplementary Information (Supplementary Fig. 1 and Supplementary Video 1). Briefly, the biomaterial is encapsulated between two polymer layers—one impermeable and one porous—with the latter interfaced and fixed on the epicardial surface of the heart. The assembled reservoir is then connected to a subcutaneous port through an implanted refill line, allowing for localized, targeted therapy to the diseased tissue (Fig. 1c). The resulting device is flexible and foldable (Fig. 1d) and can be guided through a 14G needle or 1.6 mm diameter catheter (Fig. 1d and Supplementary Video 2), lending itself to minimally invasive delivery via sub-xiphoid

puncture or a mini-thoracotomy for future translation to humans. Re-administration of therapy is achieved non-invasively through the port (Supplementary Video 3).

Pre-clinical implementation of the Therepi system. Next, we introduce a surgical method of implantation in a rat model that enables repeated replenishment of therapy from a subcutaneous port located on the back of the rat. For this pre-clinical model, the Therepi was implanted through a thoracotomy, and not minimally invasively as envisioned for translational use. A detailed description of the surgical method is described in the Supplementary Information (Supplementary Figs. 2–4 and Supplementary Video 4). In brief, in an anaesthetized rat model, the refill line was tunnelled subcutaneously from a dorsal incision to a thoracotomy. Next, an MI model was created by permanently ligating the left anterior descending (LAD) coronary artery. The Therepi reservoir was then sutured to the epicardium at the infarct border zone, and the refill line was attached to a subcutaneous, self-sealing port at the dorsal access site and closed. This allowed non-invasive, replenishable, targeted delivery, and localized release of various agents (Fig. 2a,b).

Localized delivery of small molecules. First, we confirmed that the Therepi system enables the delivery of small molecules. The imaging substrate D-luciferin was used as an analogue to demonstrate rapid, targeted delivery of small molecules to the heart. For this experiment, we used a simplified version of the Therepi system (Supplementary Fig. 2), where we directly sutured a disc of GelMA onto the epicardium (without the encapsulating TPU/polycarbonate layers) and attached a refill line and port (Supplementary Methods and Supplementary Fig. 3). The GelMA disc was pre-seeded with luciferase-expressing mouse mesenchymal stem cells (mMSCs) before implantation, such that bioluminescence of the cells indicates the presence of D-luciferin. Direct delivery via the port produced a more rapid and intense bioluminescence, as compared to systemic intraperitoneal (IP) delivery (Fig. 2c). The total dose of delivered substrate via the port was >70-fold less than the amount delivered systemically. However, delivery to the target, as evidenced by the bioluminescence (Fig. 2d) and calculated by the area under the curve normalized by the dose, was dramatically enhanced with direct delivery (Fig. 2e). To further illustrate the functional response to small-molecule delivery, epinephrine was delivered through the Therepi system while recording blood pressure with an apically inserted pressure–volume catheter. This produced a more pronounced and rapid increase in blood pressure as compared to IP delivery, as indicated by the end-systolic pressure measured over time (Fig. 2f), and the typical pressure waveforms for the first 100 seconds, recorded in the left ventricle (Fig. 2g). Notably, epinephrine delivery with the Therepi system was in an MI model where the Therepi system had been implanted for 28 days, demonstrating that epinephrine can penetrate through any fibrous capsule that may have formed around the Therepi device.

In vitro demonstration that cells remain localized, release paracrine factors into surrounding media and can be replenished. To demonstrate that seeded cells remain in the Therepi reservoir, we delivered 1 million firefly-luciferase-expressing mMSCs to the Therepi system on day 0. The system was then submerged in media in a cell culture flask, with the semi-permeable membrane in direct contact with the surface-treated base of the flask (Fig. 3a). Red firefly-luciferase (F-luc) is an intracellular protein (that is not secreted from the cells) that causes bioluminescence in the presence of oxygen and luciferin, thus acting as a proxy for cell number and location. The cells in the reservoir demonstrated F-luc activity over 28 days, quantified by bioluminescence, indicating sustained viability, and therefore transport of nutrients and waste products across the membrane (Fig. 3b). The addition of D-luciferin to the media demonstrated that cells remained in the Therepi reservoir and did not migrate out into the surrounding tissue culture flask over 28 days (Fig. 3c, sealed Therepi). We compared this to an unsealed Therepi device, which allowed cell migration out into the culture flask by day 28 (Fig. 3c, unsealed Therepi).

Next, 0.5×10^6 million Gaussia-luciferase (G-luc)-expressing mMSCs were seeded along with 0.5×10^6 F-luc mMSCs into the Therepi system at day 0 and maintained in a Therepi system submerged in media in a cell culture flask for 28 days. Unlike F-luc, which remains intracellular, G-luc is secreted from expressing cells over time (Fig. 3d). While the F-luc signal confirmed that the transplanted cells remained localized (similar to data shown in Fig. 3b, sealed Therepi), a measurement of G-luc activity in media sampled at different time points showed a constant increase in paracrine factor activity over time (Fig. 3e). This finding supports the possibility of implanted cells acting as indwelling paracrine factor sources, releasing factors that diffuse out of the reservoir.

Finally, refilling the Therepi system with cells in situ was demonstrated. 10^6 F-luc mMSCs were pre-seeded on the GelMA biomaterial and inserted into the Therepi system. At days 7 and 14, 10^6 additional cells were added to the system through the refill line, demonstrating the feasibility of multiple cell refills (Fig. 3f,g).

Transport of macromolecules through the Therepi system and fibrous capsule into tissue. To explore the transport of macromolecules through the Therepi device, fluorescently labelled bovine serum albumin (Vivotag 800, Perkin Elmer) was delivered to the heart via the Therepi system. After 3 h, there was a sustained concentration of the protein at the target site. The same dose was injected into the IP space as a control, but an undetectable quantity of the therapy had reached the target site after 3 h (Fig. 4a,b). To demonstrate that macromolecules delivered via Therepi could penetrate myocardial tissue more than 28 days post-implantation in an MI rat model, a micro-computed tomography (μCT) analysis was performed 12 h after delivery of a drug analogue (the contrast agent phosphomolybdic acid) (Fig. 4c,d). The 3D reconstruction of the excised heart enabled visualization of the distribution and penetration of delivered therapy in heart tissue. Real-time measurements of macromolecule diffusivity were obtained using a diffusion chamber consisting of two compartments separated by the tissue of interest; in this case, heart tissue explanted at various time points with a fibrous capsule of acute or chronic nature, and the polycarbonate membrane of the Therepi system (Fig. 4e). Diffusion of 40 kDa FITC-dextran is slower by a factor of ~1.7 once a fibrous capsule has formed around the membrane (Fig. 4f). After 20 days of Therepi placement, the diffusion of 10 kDa FITC-dextran through the tissue of interest is 5-fold faster than the diffusion of 40 kDa dextran, due to the lower molecular weight (Fig. 4g). Despite the formation of a fibrous capsule, which hinders diffusion to an extent, molecules with a range of molecular weights can be transported through the membrane into the tissue. A summary of this data, including tissue thickness, lag time and the diffusion coefficient, is included in Supplementary Table 1.

Next, the transport of proteins through the Therepi and the surrounding fibrous capsule was demonstrated. Fluorescently labelled bovine serum albumin (Cy7-labelled, Nanocs) was delivered through the Therepi system, 26 days post-implantation in an MI model, and after formation of a fibrous capsule. 24 h post administration, fluorescent protein had diffused from the device, and penetration through the fibrous capsule into the heart tissue was evident (Fig. 4h).

Demonstration of cell refill in vivo. The ability to deliver and replenish cells in Therepi devices placed on a rodent heart was tested. 10^6 F-luc MSCs were pre-loaded into a methacrylated gelatin

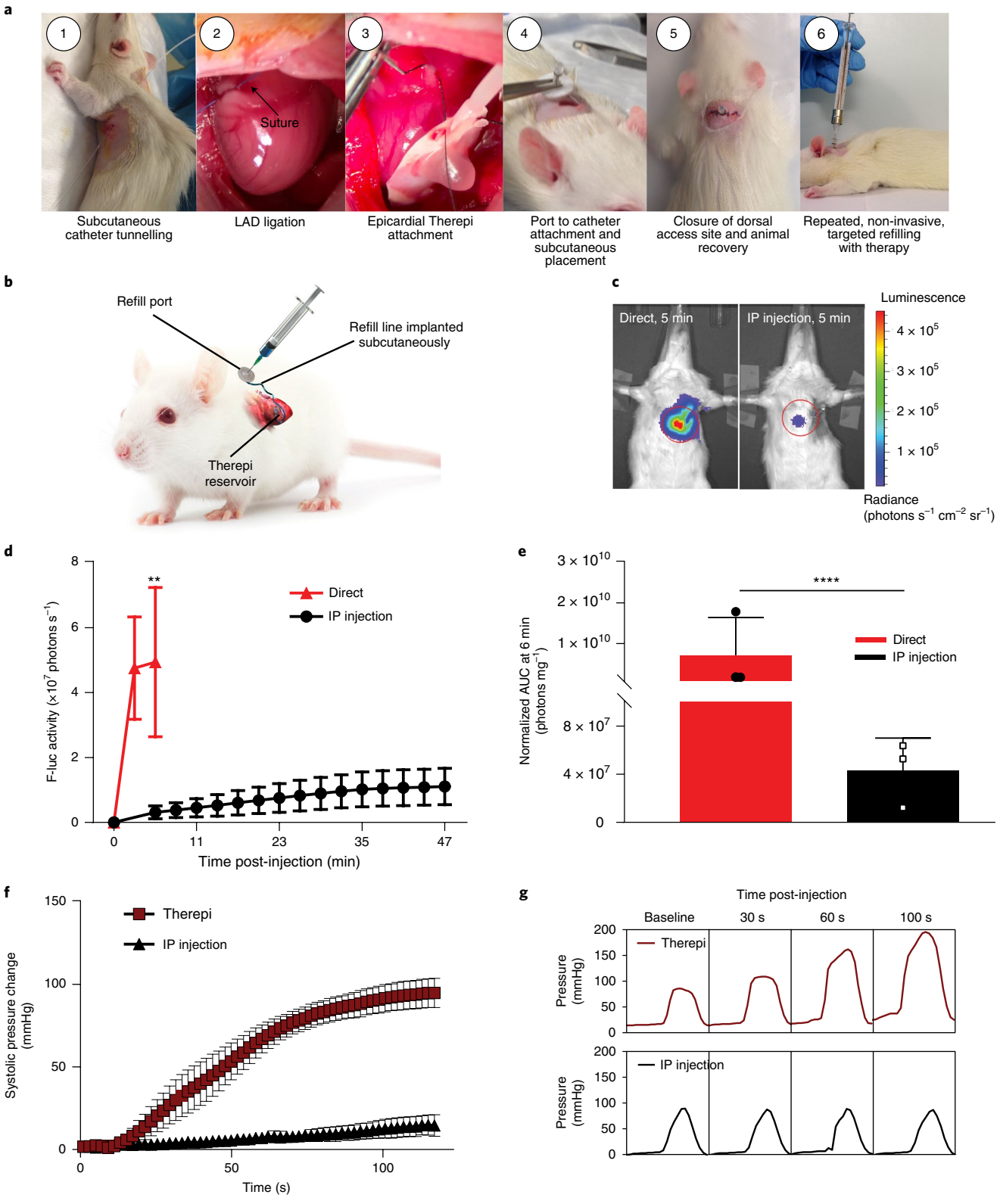

Fig. 2 | Pre-clinical implementation and demonstration of targeted small-molecule delivery. a, The surgical procedure for Therepi implantation in a rat MI model. LAD, left anterior descending coronary artery. **b**, A schematic of Therepi in a small animal model. **c**, Representative bioluminescence of D-luciferin delivery to a simplified Therepi system (direct) compared to IP injection. Circles denote the region of interest. **d**, Quantification of bioluminescence over time after injecting D-luciferin ($n = 5$). $^{**}P = 0.0011$, unpaired, two-tailed t-test between groups at 6 min. Mean values are shown and error bars are ±s.d. **e**, Area under the curve (AUC), normalized by injected weight for IP versus direct delivery of D-luciferin at 6 min. $^{****}P < 0.0001$, two-tailed, unpaired t-test. Mean values are shown, and error bars represent ±s.d. **f**, End-systolic pressure, as measured by an apically inserted pressure–volume catheter into the left ventricle post-injection of epinephrine ($n = 3$ animals). Mean values are shown and error bars are ±s.d. **g**, Typical intraventricular pressure waveforms seen with each model immediately following epinephrine injection.

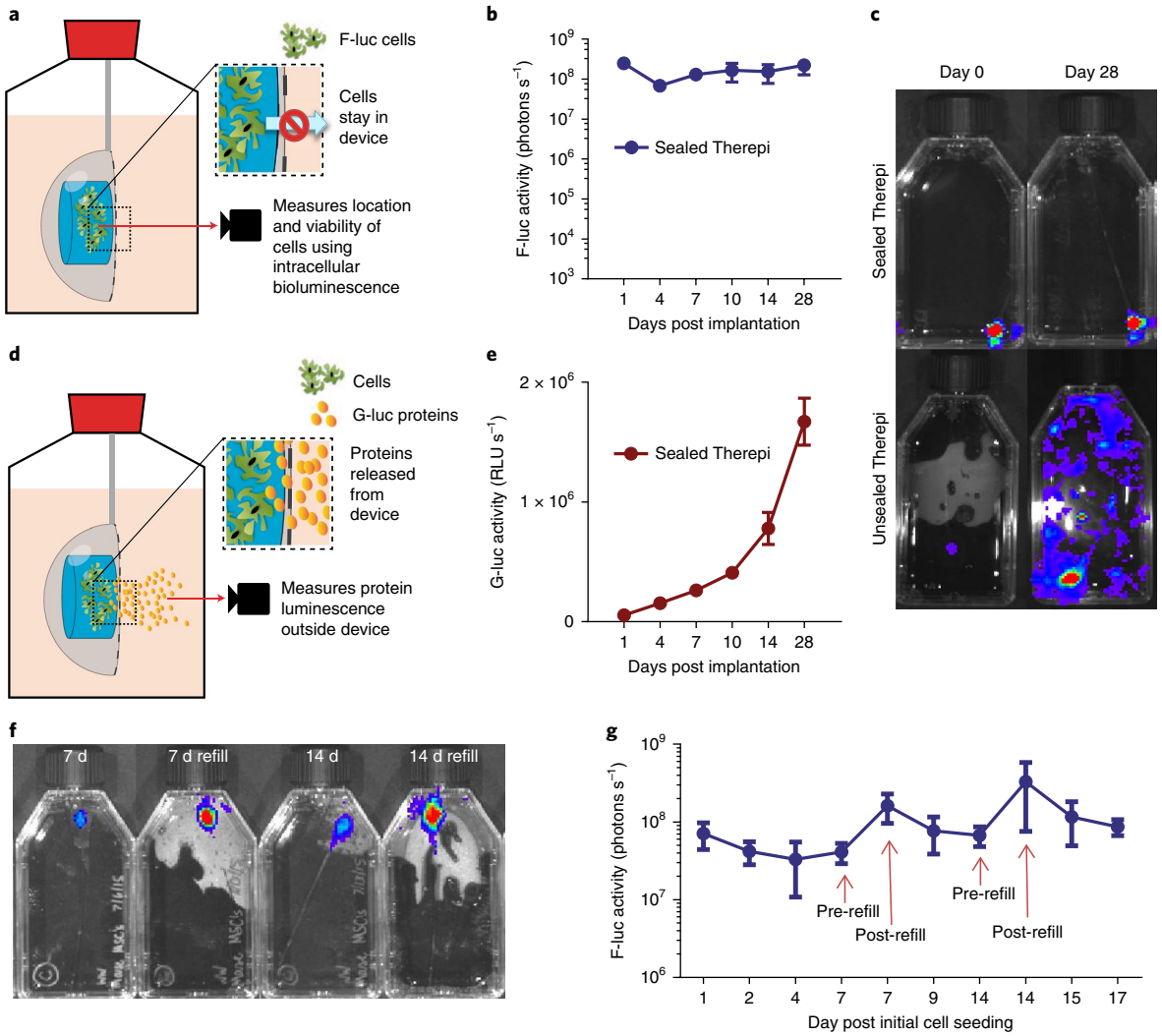

Fig. 3 | The Therepi system allows for sustained viability, cell localization, protein release and cell refills in vitro. a, A schematic of the experimental set-up used to demonstrate in vitro cell localization in the Therepi device. **b**, Luciferase activity in the sealed Therepi reservoir, showing that implanted cells remain viable in the device for up to 28 days. **c**, An IVIS image showing the location of cells via bioluminescence in a sealed and an unsealed Therepi device at day 0 and day 28. The experiment was successfully repeated 5 times. **d**, A schematic of the experimental set-up used to demonstrate in vitro protein release. While cells remain inside the device up to 28 days post-implantation, paracrine factors (measured via G-luc bioluminescence) may be released into the surrounding media. **e**, G-luc activity in the media up to 28 days. **f**, Representative bioluminescence of F-luc cells in the Therepi reservoir before and after cell refill at days 7 and 14. The experiment was repeated 5 times. **g**, Bioluminescence of F-luc cells in the Therepi reservoir with cell refills at days 7 and 14. For **b**,**e**,**g**, mean values are shown and error bars are ±s.d. ($n = 5$ devices).

cryogel (the simplified Therepi device), and at day 4, an additional 10^6 cells were refilled onto the biomaterial through the subcutaneous port. Representative bioluminescent images are shown for the refill and non-refill groups at post-operative time points (Fig. 5a). This refilling resulted in a greater than 10-fold increase in the bioluminescence, representing the number of cells at the target site, as compared to non-reloaded Therepi devices (Fig. 5b). The area under the curve for each group was calculated after background subtraction (Fig. 5c), showing a significant difference between the 'dose' of cell therapy for the refill group.

Demonstration of left ventricle functional improvement with Therepi-based cell refilling. Finally, the impact of Therepi-based cell refilling was determined in a 28-day study comparing cardiac function of the following groups over time: (1) sham (MI only), (2) a single injection of cells, (3) Therepi without any cells, (4) Therepi with cells and (5) Therepi with cells and refills (Fig. 6a). The delivered cargo was syngeneic bone-marrow-derived MSCs. Echocardiography was conducted at days 0, 7 and 28 in all groups, and for the refill group, cells were replenished at days 4 and 14 (Fig. 6b). Systolic and diastolic echocardiographic measurements were used to calculate ejection fraction (Supplementary Fig. 5a–c). Ejection fraction and fractional shortening tended to decrease over time for the MI-only and the cell injection groups, but increased over time for the acellular Therepi device, and significantly for the Therepi with cell refill (Fig. 6c–e). Additional day 7 and day 28 ejection fraction significance comparisons are shown in Supplementary Fig. 5d,e. Haemodynamic measurements of these animals were obtained with a pressure–volume (PV) catheter (AD instruments) at day 28 as described in Fig. 6f–h, the Supplementary Methods and Supplementary Video 5. Representative PV loops for the MI-only and Therepi with cell refill regimes are shown in Fig. 6f and indicate a leftward shift, and an increase in stroke work (area of PV loop). PV-based ejection fraction measurements agreed with the echocardiographic measurements (Fig. 6g) and stroke work demonstrated similar trends (Fig. 6h) with Therepi with repeated cell dosing

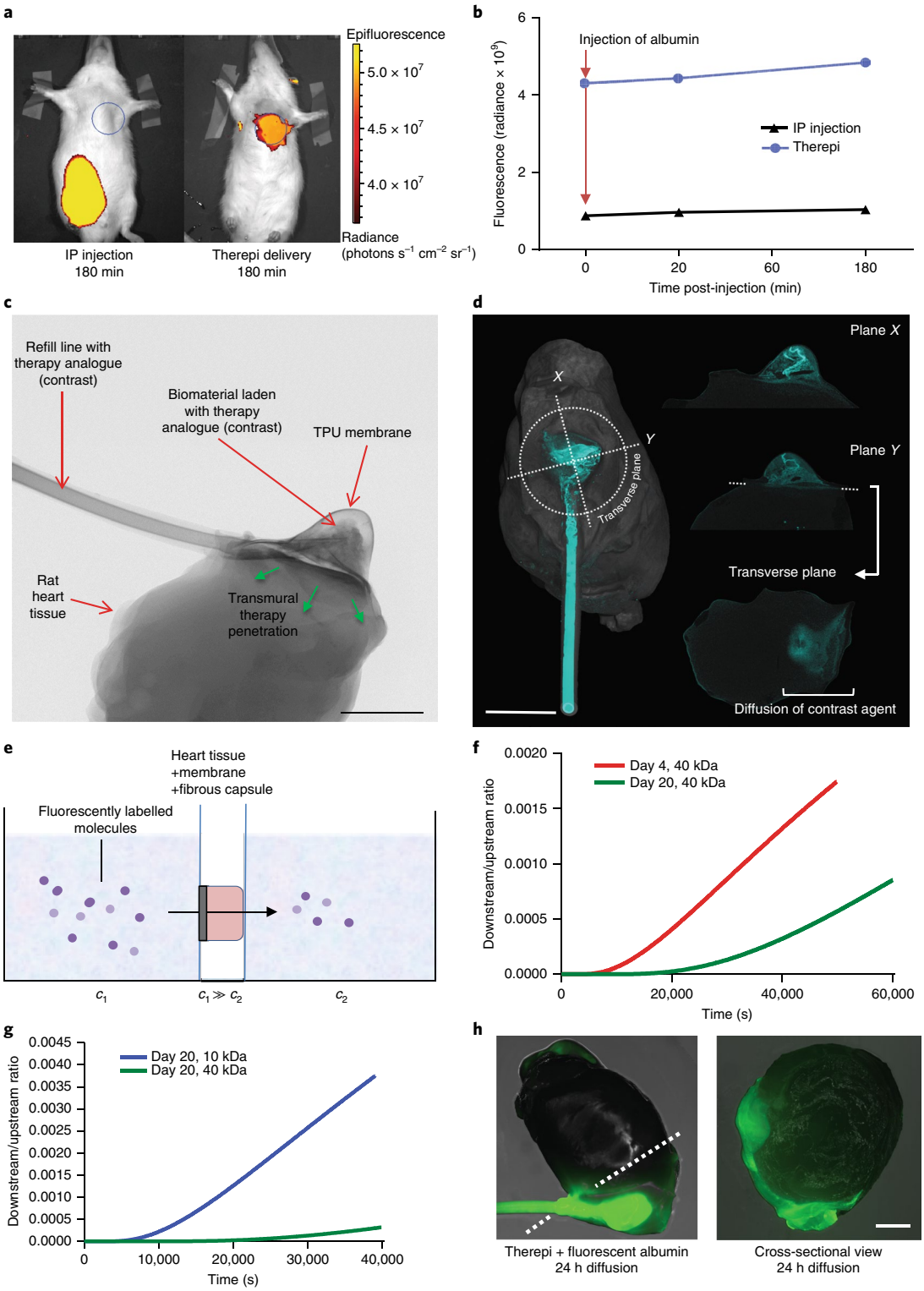

Fig. 4 | Demonstration of fibrous capsule penetration and 3D distribution of macromolecules in the myocardium. a, Fluorescent images from the IVIS, showing two rat models 3 h after fluorescently labelled bovine serum albumin was injected into the Therepi system or into the IP space. Circles denote the region of interest. **b**, Quantification of fluorescence at the heart at specific time points following Therepi or IP albumin injection. **c**, An image from the μCT scanner showing the Therepi reservoir on the explanted heart and the direction of PMA contrast agent (therapy analogue) penetration. **d**, 3D reconstruction of entire CT scans at two orthogonal planes and the transverse plane. **e**, A schematic of the diffusion chamber. c_1 is the concentration of solute in the upstream chamber, and c_2 is the concentration of solute in the downstream chamber. **f**, Diffusion of fluorescently labelled 40 kDa dextran over time through the diffusion chamber, for devices previously implanted for 4 or 20 days. **g**, Diffusion of 10 kDa and 40 kDa dextran across fibrous capsules resulting from implantation for 20 days. **h**, Diffusion of fluorescent albumin through the fibrous capsule into the heart tissue, 24 h post-delivery of Cy7 (cyanine-7)-labelled albumin. Left: merged fluorescent and bright-field images of the explanted heart + Therepi device 26 days after surgical implantation. The heart was cut at the white dotted line. Right: merged fluorescent and bright-field images of a cross-section (indicated by the white dotted line). For **a**,**c**,**d**, and **h**, each experiment was performed once for visualization purposes. Scale bars (**c**,**d**,**h**), 4 mm.

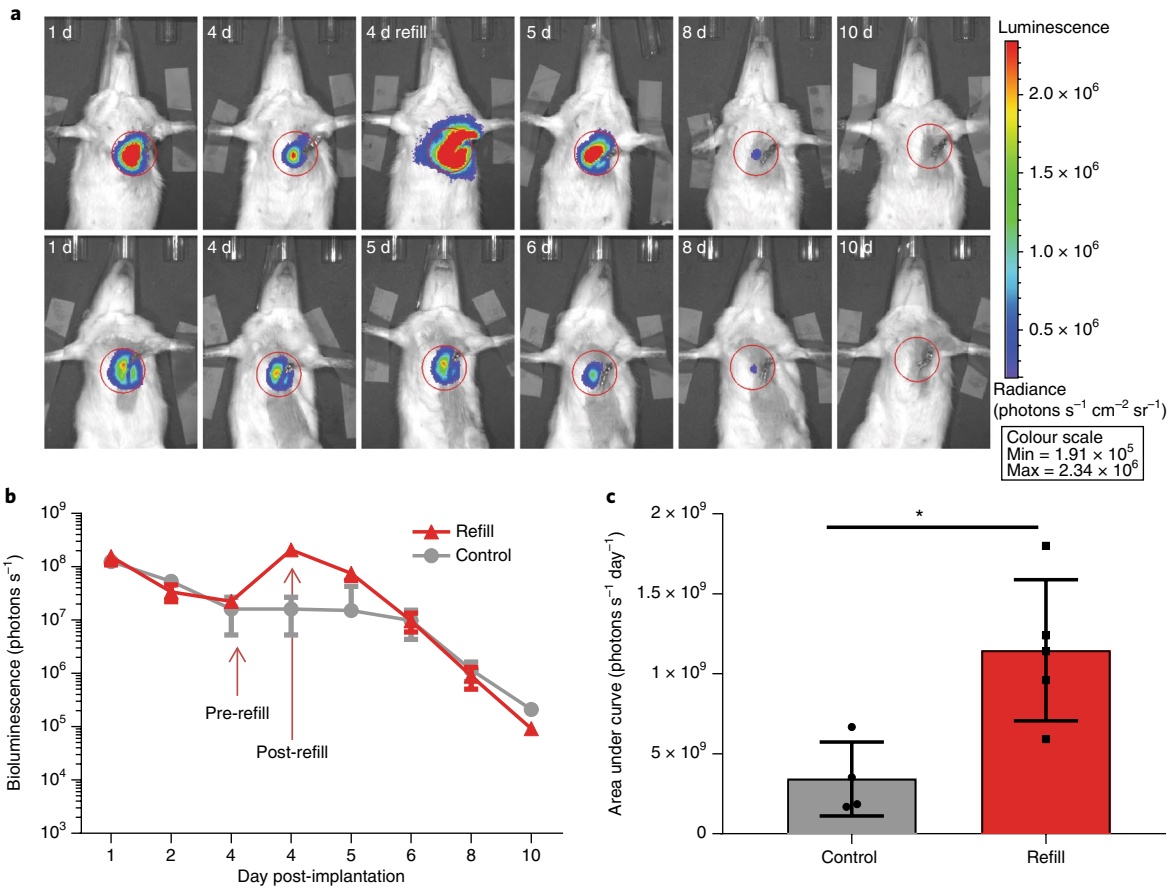

Fig. 5 | Cell refill from the simplified Therepi device in vivo. a, Representative IVIS images of typical F-luc-derived bioluminescence at various time points for the control group and the refill group, with refill at day 4. Circles denote the region of interest. **b**, Quantified bioluminescence following administration of D-luciferin at various time points. Mean values are shown and error bars are ±s.d. **c**, AUC for the groups with and without refill; background bioluminescence was subtracted. Mean values are shown. Error bars are +s.d. * $P = 0.0136$, $n = 4$ or 5 animals; two-tailed, unpaired t-test.

showing superiority to the no-treatment group. The finding that cell refills at later time points provided functional benefit suggests therapeutic agents released from the device can diffuse into adjoining cardiac tissue.

Histological analysis. Samples of tissues from the in vivo MI rat model at 28 days were stained with H&E, and analysis was conducted by a cardiac/medical device pathologist (Fig. 7). The gross appearance of the Therepi device at day 28 on the heart is shown in Fig. 7a, with the device conforming to the heart. Histological slices were taken through the device and heart in a transverse slice (Fig. 7b). A histological overview of the Therepi device demonstrates the TPU layer, polycarbonate membrane, enclosed Gelfoam and reservoir contents, as well as the fibrous capsule, is evident at the device/epicardial interface (Fig. 7c) (note that the breach in the TPU layer here is a processing artefact). The fibrous capsule for the Therepi device in the presence or absence of cells and with cell replenishments had a similar appearance and thickness (Fig. 7d–f). Histological examination of the Therepi reservoir in the absence of transplanted cells demonstrates there is no matrix or tissue laid down with the Gelfoam (Fig. 7g). Conversely, in the presence of transplanted cells, a cell-derived matrix is laid down by the MSCs in the reservoir (Fig. 7h,i). If the seal of the Therepi is breached, there is a significant foreign body response, including macrophages, giant cells and vascularization within the Therepi reservoir, which is not seen with the intact Therepi (Fig. 7i).

Discussion

Recent publications have indicated that "repeated dosing has the potential to be a disruptive advance that may revolutionize cell therapy"[5]. In addition to cells, repeated dosing is likely to improve benefit with other therapeutic technologies, such as growth factors[3–10] and small molecules[11–16], motivating our current work. We present an implantable reservoir system that allows targeted, replenishable and sustained presentation of molecular and cellular therapy to the heart. The ability of the Therepi system to allow targeted injection of molecular therapies directly to the heart was demonstrated by delivering D-luciferin through the subcutaneous port. Transport of molecules out of the Therepi system and into the surrounding tissue (even after 28 days in vivo and formation of a fibrous capsule) was demonstrated for bioagents of a range of sizes including epinephrine, dextran and albumin. We also demonstrated repeated delivery of cells through the port at discrete time points, increasing the resident cell number by 10-fold. To enable a sustained cell infusion, the reservoir could be connected to a small implanted, refillable pump[13,16] (for example, Bio Leonheardt's stem cell pump, www.bioleonhardt.com).

Localized delivery to the epicardium and pericardial sac using the Therepi system could potentially improve drug efficiency, thereby requiring lower doses and reducing adverse off-target effects. This is a particularly important issue for drugs with a narrow therapeutic index, where a high concentration when given by traditional systemic routes could cause toxic side effects, while a low concentration could eliminate any clinical benefit. The efficacy

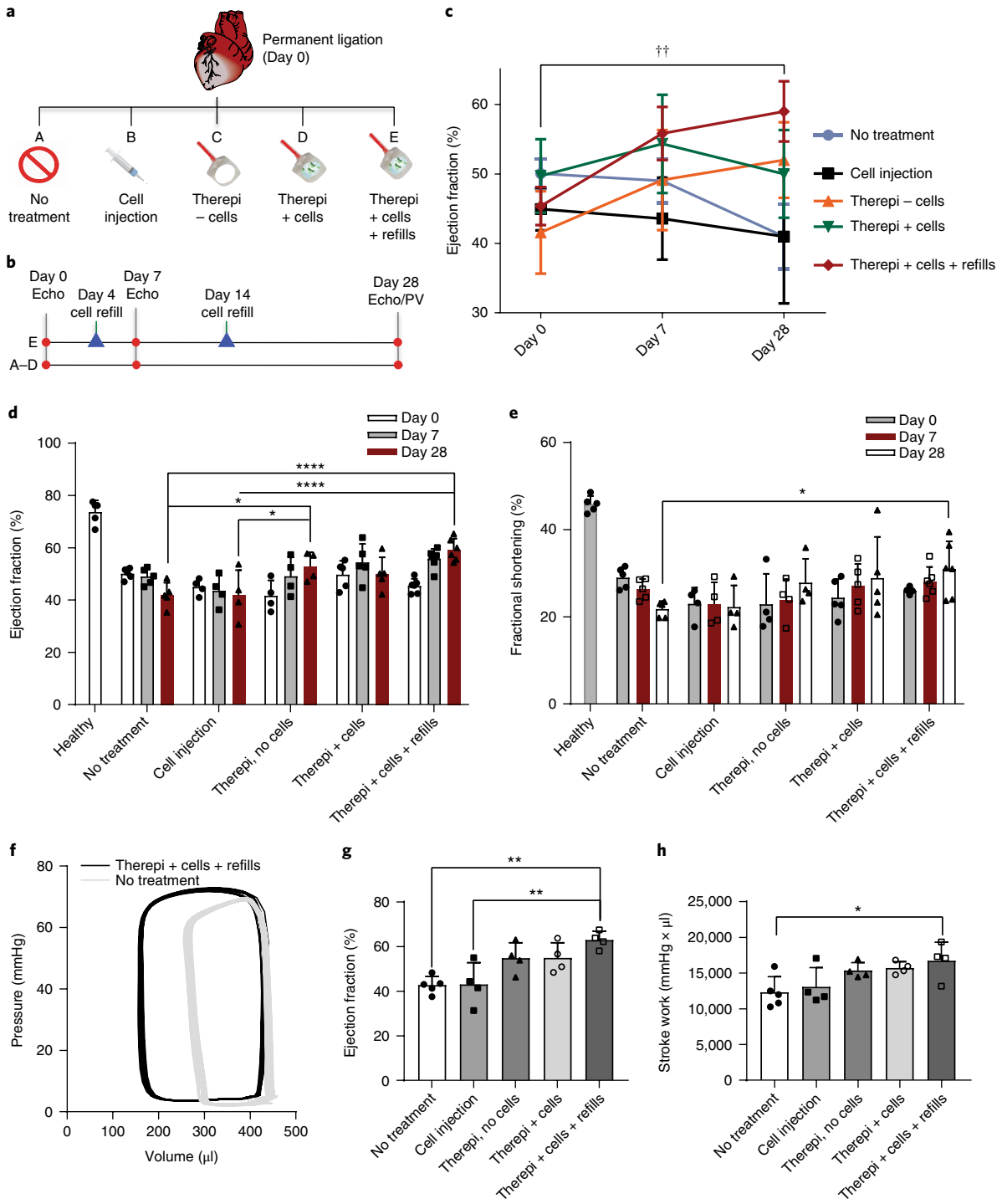

Fig. 6 | Pre-clinical safety and efficacy of the replenishable cell delivery device. a, A description of groups for the 28-day pre-clinical study. **b**, A timeline for the pre-clinical study, including timing of cell refills. **c**, Ejection fraction over time assessed by echocardiography where $^{\dagger\dagger}P < 0.003$ is the significance for the Therepi + cells + refill group between days 0 and 28. Mean values are shown and error bars are ±s.d. ($n = 4$–6), as analysed by a two-way analysis of variance (ANOVA) across time points for each treatment group. **d**, Ejection fraction for all groups as assessed by echocardiography. $^{*}P < 0.05$, $^{****}P < 0.0001$; see Supplementary Table 2 for exact P values. Mean values are shown and error bars are +s.d. ($n = 4$–6 animals), as analysed by a two-way ANOVA, with Tukey's multiple comparisons post-test. **e**, Fractional shortening for all groups assessed by echocardiography. Mean values are shown and error bars are +s.d. ($n = 4$–6 animals), as analysed by a two-way ANOVA. $^{*}P = 0.0228$. **f**, Representative PV Loops for Therepi + cells + refill compared to MI with no treatment. **g**, Ejection fraction for all groups as assessed by haemodynamic measurements. $^{**}P = 0.002$ (versus no treatment), $^{**}P = 0.0037$ (versus cell injection). Mean values are shown and error bars are +s.d. ($n = 4$ or 5 animals), as analysed by a one-way ANOVA. **h**, Stroke work for all groups assessed by haemodynamic measurements. $^{*}P = 0.0382$. Mean values are shown and error bars are +s.d. ($n = 4$ or 5 animals), as analysed by a one-way ANOVA, with Tukey's multiple comparisons post-test.

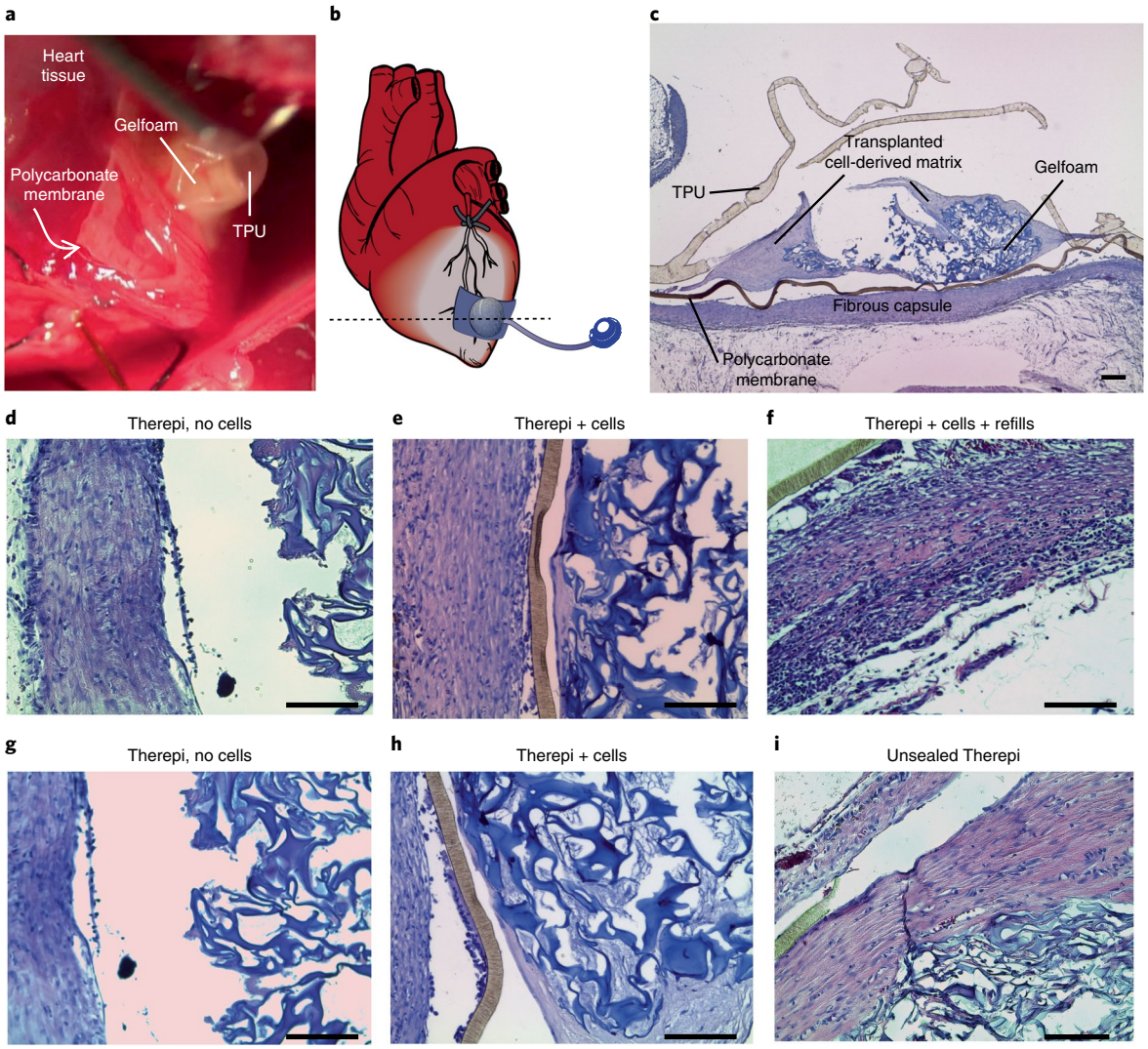

Fig. 7 | Histological analysis of the Therepi device in vivo. a, Appearance of Therepi on the heart after 28 days. Similar gross results were seen in all 15 implanted devices. **b**, A schematic of the section through the device taken for histology. **c**, An overview of the histological appearance of Therepi (TPU and polycarbonate membrane are visible, as well as the Gelfoam with transplanted cells, and the fibrous capsule). **d**–**f**, Histological images of the device/heart interface, showing a similar fibrous capsule for each Therepi group, regardless of the presence of cells. **g**–**i**, Histological images showing very few cells and no cell-derived matrix, foreign response or vascularization in the Gelfoam in the absence of transplanted cells, indicating the immune protection imparted by the Therepi system (**g**). In the presence of transplanted cells (**h**), transplanted-cell-derived fibrous tissue integrated with the Gelfoam. As a control, a histological image from an unsealed Therepi device shows a foreign body response, including vascularization, macrophages and giant cells (**i**). Scale bars, 100 µm. For **c**,**e**,**f**,**h**, the experiment was performed once. For **d**,**g**,**i**, the experiments were repeated twice with similar results.

of epicardial drug delivery has been studied for angiogenic substances[44] and vasodilators[14], as well as anti-arrhythmic agents[45,46], but easy and continuous access to the epicardial surface has been a major limiting factor. The Therepi system may allow the clinical translation of this type of therapy and, potentially, enable delivery to other diseased tissues.

This work was completed using two gelatin-based biomaterials (GelMA and Gelfoam). Both forms of sponge contain large, interconnected pores, and diffusion would be expected to be unimpeded through them[42]. Gelatin is derived from collagen and contains inherent peptide sequences that facilitate cell adhesion and enzymatic degradation. Due to its low cost, lack of immunogenicity, and previous use in medicine as a haemostatic agent and blood volume expander, it is an attractive implantable biomaterial. However, we foresee that this technology can be extended to other biomaterials that have demonstrated an ability to increase cell retention at the heart (such as alginate[33], chitosan[31], hyaluronic-acid-based gels[26,36] and collagen[2,43]). The delivered cargo was a syngeneic MSC derived from the bone marrow of Sprague Dawley rats. A stem cell originating from bone marrow was chosen for the following reasons: (1) there is pre-clinical evidence for it improving left ventricular function[47–49], (2) it has already been used extensively in cardiac regenerative human trials, where feasibility of cell isolation and safety of the cells following delivery were established[50–52], and (3) it has demonstrated attractive cell therapeutic potential for a range of diseases characterized by chronic inflammation[53].

Given the poor survival and rapid clearance of cells post administration, repeated doses are likely to be needed for best efficacy (similarly to most pharmacological medications)[38]. Proposed effects following cell delivery are multifactorial and include induction of cardiac muscle cell proliferation, immobilization of resident stem cells, neovascularization, inhibition of apoptosis, and immunomodulation[54]. It is envisaged that each cell delivery will result in a bolus release of intracellular contents including cytokines, chemokines,

exosomes and paracrine factors, followed by a lower sustained release until loss of stemness or cell death. Importantly, a cumulative benefit following repeat delivery has been demonstrated with two different cell types, c-kit^{POS} cardiac progenitor cells[37] and cardiac mesenchymal cells[55]. Interestingly, the acellular Therepi provided a sustained benefit across the 28-day study, potentially due to its mechanical reinforcement of the remodelling ventricle or due to an altered healing response caused by the foreign body response. Early mechanical restraint of the infarcted left ventricle with polymeric meshed materials or wraps has been demonstrated to be highly effective in reducing infarct expansion and limiting negative remodelling in large animal pre-clinical models[56–58]. However, the Therepi with one-time cell delivery had poor results, despite providing mechanical reinforcement. While this is surprising, it highlights the importance of cell delivery timing for positive modulation of the post-MI healing response. The harsh inflammatory environment of the infarcted heart has been shown to drive delivered MSCs towards a pro-inflammatory phenotype, limiting their reparative efficacy[59]. Cells delivered at the time of MI, and their secretome, would have been subject to this environment, and may even have adversely affected healing and negated any positive effect from the device mechanical reinforcement. If later delivery of cells is favourable, the Therepi system can be advantageous in allowing implantation of an acellular device, followed by subsequent cell delivery at a later time point, as described for other applications[60]. This approach would complement delivery with autologous stem cells[61], when, for example, a biopsy could be taken at the time of implantation of the Therepi, and stem cells would be isolated, expanded and then re-implanted through the Therepi device after a number of weeks or months without the need for an additional surgery.

To maximize the potency of cell therapy, immune protection of transplanted cells would be beneficial. The histological data for the pre-clinical study shown here supports the idea that the Therepi system, when intact, imparts immune protection to the enclosed cargo. This prevents cell infiltration and a significant foreign body response around the gelatin-based biomaterial, as seen with the unsealed Therepi system. An immune response of this nature is likely to have led to reduced cell viability at later time points and lessened the efficiency of cell replenishments, despite an initial large increase in cell number. Further refinement could potentially enable a greater degree of control over the transplanted cell source and allow the de novo production of paracrine factors from an allogeneic or possibly a genetically engineered cell source, without the associated safety concerns.

In addition, for pre-clinical models, systems that can longitudinally monitor viability and function of transplanted cells in vivo would be beneficial[41]. Therepi has additional use as an enhanced imaging method for quantifying cell number on the heart. In this case, the imaging substrate D-luciferin can be injected directly via the Therepi catheter to a biomaterial loaded with luciferase-expressing cells, requiring much less substrate compared to conventional IP delivery. Additionally, the need to wait for systemic distribution of D-luciferin is removed, thus reducing the time the animal is under anaesthesia. This represents a considerable advantage in terms of convenience, cost, consistency, and time taken to conduct animal imaging. Therepi can be used, if desired, for injection of media or nutrients into the reservoir to prolong cell survival. Bio-sensing molecules or components could also be injected and retrieved locally to monitor biomarkers indicative of disease. The potential of the system for monitoring and feedback is vast.

In terms of potential clinical translation, the Therepi system enables the multimodal localized delivery of different molecular therapies (cells, small molecules and macromolecules) to mimic or modify the inherently complex physiological and pathological processes in the heart. The system, with its method of implantation and ability for cell monitoring, is potentially extremely beneficial, as it could enable sustained delivery of the paracrine factors released from transplanted cells in proximity to the diseased tissue of the heart, and could allow further research studies into the effect of multiple administrations of cells that have previously been impossible due to the prohibitive nature of multiple invasive surgeries. In addition to temporal control, multiple reservoirs would enable spatial control and multimodal treatment regimens to various parts of the heart; for example, delivery of pro-regenerative therapy to the left ventricle, coupled with anti-arrhythmic therapy to the left atrium.

However, there are some potential bottlenecks that need to be overcome before clinical translation is possible. First, the route of clinical access needs to be established. Clinically, our device is intended for percutaneous pericardial access, via sub-xiphoid access and pericardial puncture. Such an approach is increasing as more interventional cardiologists and electrophysiologists become comfortable with it, presenting opportunities for intrapericardial drug delivery[62,63]. Current interventional procedures for pericardial diseases include pericardiocentesis and percutaneous balloon pericardiotomy, demonstrating utility of this route for cardiac applications[62,63]. We used sutures for device attachment in this manuscript, but recent innovations in hydrogel adhesion could be used for a less invasive and more uniform adhesion to the heart[64].The procedure could be carried out in hybrid cath labs during reperfusion and would be an addition/adjunct to the current clinical management of a patient with MI. While the intent of this device is not for delivery during open-chest surgery, patients with advanced coronary heart disease undergoing coronary artery bypass graft surgery could also be a target population.

It should be acknowledged that standard procedures for cell delivery to the heart, including transendocardial and intracoronary catheter delivery (via femoral access), are less invasive in comparison with Therepi, and do not require general anaesthesia. However, Therepi would be a one-time implantation that allows for multiple therapy administrations, which could be done in an ambulatory setting. Furthermore, the biomaterial reservoir would vastly extend cell survival, and thus potential clinical benefit, in comparison to a cell injection alone. Minimizing pericardial adhesions will also be important. Minimally invasive catheter delivery could reduce post-procedural pericarditis, and therefore adhesions, in comparison with open-chest surgery. Alternative methods for reducing pericardial adhesions have also been reported, such as pharmacological control of inflammation (using corticosteroids) and enzymatic breakdown of fibrous tissue (using fibrinolytics)[65]. Localized delivery of these agents could be possible via Therepi.

Second, catheter-associated infections could be a potential issue. It is worth noting, however, that a permanent pericardial drainage system connected to a subcutaneous port has previously been safely implanted in patients for up to 5 weeks, with no infection noted[66]. Moreover, a multicentre randomized control trial is currently being undertaken to determine the safety and efficacy of extended pericardial drainage in comparison to a one-off pericardiocentesis procedure[67]. A fully subcutaneous port with a self-sealing septum could be used to minimize the risk, and ports are already widely used for other applications, such as central venous access for chemotherapy drugs. The catheter tubing could be surface modified with an antibacterial or with hydrophilic coating to reduce bacterial adherence. Depending on the length of implantation/use, it is likely that a broad-spectrum prophylactic antibacterial regimen will be needed. In the event of disease resulting from the implantation, such as purulent pericarditis, the Therepi system itself could be used for the intrapericardial delivery of antibacterials and fibrinolytics.

Third, the fibrous capsule at the Therepi/heart interface could affect transport of therapy into the tissue, and this effect should be further studied. We have initially demonstrated that, despite the formation of a fibrous capsule (which hinders but does not impede diffusion), molecules with a range of molecular weights can be transported through the membrane into the tissue. Furthermore,

we noted a clear functional effect through the Therepi 28 days after implantation. This functional benefit shown with later refills of cells support that paracrine factors can diffuse through this capsule. Future iterations of the device could use microneedle technology to allow for direct injection into tissue. Fourth, MRI compatibility would be advantageous. Current materials are all MRI compatible, except for the port, which would require modification. Fifth, it is important to design the system with mechanisms to avoid catheter obstruction by therapies, such as cell debris. In this study, cells were removed from the line by following each dose with saline, to clear the line. Other approaches could include enzymatic degradation and mechanical suction. Future versions of Therepi could be designed with a dual loop system to aid with these solutions.

Future work before clinical implementation will focus on biodegradable device development so there is no foreign material remaining on the heart. A permanent version of the device could also be an option, allowing for acute therapy replenishments initially and taking advantage of the long-term passive reinforcement effects[68].

It should be noted that in this pre-clinical study we initiated treatment immediately after the time of cardiac injury. This is not directly clinically relevant, as cardiac injury would precede device implantation in the clinic. Future work will involve testing this device subsequent to injury. Furthermore, one type of cell cargo was tested here, a syngeneic mesenchymal cell source. There is a plethora of available cell sources, and other therapeutic cargos available. Determining the correct cargo, dose and administration frequency, along with an accompanying mechanism of action, will be key to advancing this delivery concept to the clinic[38].

We can draw six conclusions from this study. (1) Implantation of the Therepi on a heart with a conduit connecting the reservoir to a subcutaneous access port is possible in a rat model. (2) The system enables direct, potent delivery of small molecules, which can elicit a functional effect and can also be used for delivery of substrates for in vivo imaging. (3) The system enables localized delivery of macromolecules that penetrate through the fibrous capsule into the myocardial tissue and distribute in three dimensions. (4) Non-invasive replenishment of cells is possible in vivo and improves cell number at the target site. (5) In a 28-day rodent study in an MI model, the Therepi device (acellular or with transplanted cells) demonstrates therapeutic superiority compared to no treatment or a single cell injection, and this effect is increased with repeated cell administrations. (6) The implanted system constitutes a rapid, inexpensive and safe method for bioluminescent quantification of cell number by direct administration of imaging substrate during in vivo imaging.

Methods

An expanded methods section is included in the Supplementary Information and includes more details on GelMA synthesis, Therepi fabrication, μCT imaging, in vitro and in vivo studies, histology and statistical methods.

Therepi fabrication. The fabrication methods for the Therepi system are shown in Supplementary Fig. 1 and described in Supplementary Methods. Briefly, a TPU sheet (HTM 8001-M polyether film, 0.003 inch thick, American Polyfilm, Inc) was formed into a hemispherical reservoir using a vacuum thermal former (Yescom Dental Vacuum Former, Generic). This was then heat sealed to a second TPU layer with a 4 mm circular window, using a heat transfer machine (Heat Transfer Machine QXAi, Powerpress). The assembly was sealed to a polycarbonate membrane, Cyclopore Track-Etched Membrane Filter (13 mm diameter, 0.4 μm, Whatman) using an impulse heat sealer (H-2065 Deluxe Impulse Sealer, Uline). One edge was left open for subsequent biomaterial insertion. The neck of the reservoir was heat bonded to a 10 cm, 3 Fr thermoplastic polyurethane catheter (Micro-Renathane 0.037" x 0.023, Braintree scientific). The assembly was sterilized in a low temperature ethylene oxide cycle and the final manufacturing steps were aseptically conducted in a class II laminar flow hood. A disc of biomaterial, either dehydrated GelMA or Gelfoam, was inserted into the reservoir and the remaining open edge was sealed.

In vivo studies. *Animal surgery for the MI model and Therepi system implantation.* Animal procedures were reviewed and approved according to ethical regulations by the Institutional Animal Care and Use Committees at Harvard University and Brigham and Women's Hospital respectively. All surgical procedures are described in Supplementary Methods. Briefly, female Sprague Dawley rats (225–250 g) were anaesthetized using isoflurane (1–3% isoflurane in oxygen). The hair between the shoulder blades and on the left side of the chest was removed. A pre-operative analgesic, buprenorphine (0.05 mg kg^{-1} subcutaneously), was administered. The regional nerve blocker lidocaine/bupivacaine was injected subcutaneously at the surgical sites. Endotracheal intubation was performed as described in Supplementary Methods. The Therepi refill line was then tunnelled subcutaneously from the dorsal site to a ventral exit site close to the left fourth intercostal space (Supplementary Fig. 2). The pericardium was removed using fine forceps. A myocardial infarction was created as previously described[43]. The LAD was permanently ligated with a suture (6-0 prolene) approximately one third of the way from the apex to the base of the heart. Myocardial blanching was apparent after ligation of the LAD, confirming infarction. The Therepi reservoir was sutured (8-0 prolene) onto the heart at the infarct border zone using the surgical guided holes placed in the device (Supplementary Methods, Supplementary Video 4 and Supplementary Fig. 3). Following Therepi placement, a vascular access button, or self-sealing port (VAB62BS/22, Instech Laboratories), was connected to the dorsal end of the catheter and placed subcutaneously between the shoulder blades of the rat (Fig. 3 and Supplementary Figs. 3 and 4). The vascular access button was secured to the underlying fascia using at least two interrupted sutures (Ethicon 4-0 vicryl). The skin was closed and the animal was ventilated with 100% oxygen on a heated pad until autonomous breathing was regained. 3 ml of warm saline was administered subcutaneously and buprenorphine (0.05 mg kg^{-1} in 50 μl IP) was given every 12 h for three days post-operatively.

Reporting Summary. Further information on experimental design is available in the Nature Research Reporting Summary linked to this article.

Data availability. The authors declare that all data supporting the findings of this study are available within the paper and its Supplementary Information. Source data for the figures are available from the corresponding authors upon reasonable request.

Received: 23 May 2016; Accepted: 9 May 2018;
Published online: 11 June 2018

References

1. O'Neill, H. S. et al. Biomaterial-enhanced cell and drug delivery: lessons learned in the cardiac field and future perspectives. *Adv. Mater.* **28**, 5648–5661 (2016).
2. Hastings, C. L. et al. Drug and cell delivery for cardiac regeneration. *Adv. Drug Deliv. Rev.* **84**, 85–106 (2015).
3. Jung, D. W. & Williams, D. R. Reawakening atlas: chemical approaches to repair or replace dysfunctional musculature. *ACS Chem. Biol.* **7**, 1773–1790 (2012).
4. Plowright, A. T., Engkvist, O., Gill, A., Knerr, L. & Wang, Q. D. Heart regeneration: opportunities and challenges for drug discovery with novel chemical and therapeutic methods or agents. *Angew. Chem. Int. Ed.* **53**, 4056–4075 (2014).
5. Segers, V. F. M. & Lee, R. T. Protein therapeutics for cardiac regeneration after myocardial infarction. *J. Cardiovasc. Transl. Res.* **3**, 469–477 (2010).
6. Segers, V. F. M. et al. Local delivery of protease-resistant stromal cell derived factor-1 for stem cell recruitment after myocardial infarction. *Circulation* **116**, 1683–1692 (2007).
7. Ziegler, M. et al. The bispecific SDF1-GPVI fusion protein preserves myocardial function after transient ischemia in mice. *Circulation* **125**, 685–696 (2012).
8. Urbanek, K. et al. Cardiac stem cells possess growth factor-receptor systems that after activation regenerate the infarcted myocardium, improving ventricular function and long-term survival. *Circ. Res.* **97**, 663–673 (2005).
9. Jabbour, A. et al. Parenteral administration of recombinant human neuregulin-1 to patients with stable chronic heart failure produces favourable acute and chronic haemodynamic responses. *Eur. J. Heart Fail.* **13**, 83–92 (2011).
10. Torella, D. et al. Cardiac stem cell and myocyte aging, heart failure, and insulin-like growth factor-1 overexpression. *Circ. Res.* **94**, 514–524 (2004).
11. Hsueh, Y. C., Wu, J. M., Yu, C. K., Wu, K. K. & Hsieh, P. C. Prostaglandin E2 promotes post-infarction cardiomyocyte replenishment by endogenous stem cells. *EMBO Mol. Med.* **6**, 496–503 (2014).
12. Saraswati, S. et al. Pyrvinium, a potent small molecule Wnt inhibitor, promotes wound repair and post-MI cardiac remodeling. *PLoS ONE* **5**, e15521 (2010).
13. van Brakel, T. J. et al. Intrapericardial delivery enhances cardiac effects of sotalol and atenolol. *J. Cardiovasc. Pharmacol.* **44**, 50–56 (2004).
14. Baek, S. H. et al. Augmentation of intrapericardial nitric oxide level by a prolonged-release nitric oxide donor reduces luminal narrowing after porcine coronary angioplasty. *Circulation* **105**, 2779–2784 (2002).

15. Waxman, S., Moreno, R., Rowe, K. A. & Verrier, R. L. Persistent primary coronary dilation induced by transatrial delivery of nitroglycerin into the pericardial space: a novel approach for local cardiac drug delivery. *J. Am. Coll. Cardiol.* **33**, 2073–2077 (1999).
16. Hermans, J. J. R. et al. Pharmacokinetic advantage of intrapericardially applied substances in the rat. *J. Pharmacol. Exp. Ther.* **301**, 672–678 (2002).
17. Laflamme, Ma, Zbinden, S., Epstein, S. E. & Murry, C. E. Cell-based therapy for myocardial ischemia and infarction: pathophysiological mechanisms. *Annu. Rev. Pathol.* **2**, 307–339 (2007).
18. Ashraf, M. et al. Systems approaches to preventing transplanted cell death in cardiac repair. *J. Mol. Cell. Cardiol.* **45**, 567–581 (2008).
19. Gavira, J. J. et al. Repeated implantation of skeletal myoblast in a swine model of chronic myocardial infarction. *Eur. Heart J.* **31**, 1013–1021 (2010).
20. Clifford, D. M. et al. Stem cell treatment for acute myocardial infarction. *Cochrane Datab. System. Rev.* **2**, CD006536 (2012).
21. Gnecchi, M. et al. Evidence supporting paracrine hypothesis for Akt-modified mesenchymal stem cell-mediated cardiac protection and functional improvement. *FASEB J.* **20**, 661–669 (2006).
22. Kinnaird, T. et al. Marrow-derived stromal cells express genes encoding a broad spectrum of arteriogenic cytokines and promote in vitro and in vivo arteriogenesis through paracrine mechanisms. *Circ. Res.* **94**, 678–685 (2004).
23. Gnecchi, M., Zhang, Z., Ni, A. & Dzau, V. J. Paracrine mechanisms in adult stem cell signaling and therapy. *Circ. Res.* **103**, 1204–1219 (2008).
24. Wang, X., Zachman, A. L., Haglund, N. A., Maltais, S. & Sung, H. J. Combined usage of stem cells in end-stage heart failure therapies. *J. Cell. Biochem.* **115**, 1217–1224 (2014).
25. Hamdi, H. et al. Cell delivery: intramyocardial injections or epicardial deposition? A head-to-head comparison. *Ann. Thorac. Surg.* **87**, 1196–1203 (2009).
26. Smith, R. R., Marbán, E. & Marbán, L. Enhancing retention and efficacy of cardiosphere-derived cells administered after myocardial infarction using a hyaluronan-gelatin hydrogel. *Biomatter* **3**, e24490 (2013).
27. Qian, L. et al. Hemodynamic contribution of stem cell scaffolding in acute injured myocardium. *Tissue Eng. Part A* **18**, 1652–1663 (2012).
28. Habib, M. et al. A combined cell therapy and in-situ tissue-engineering approach for myocardial repair. *Biomaterials* **32**, 7514–7523 (2011).
29. Christman, K. L. et al. Injectable fibrin scaffold improves cell transplant survival, reduces infarct expansion, and induces neovasculature formation in ischemic myocardium. *J. Am. Coll. Cardiol.* **44**, 654–660 (2004).
30. Singelyn, J. M. & Christman, K. L. Injectable materials for the treatment of myocardial infarction and heart failure: the promise of decellularized matrices. *J. Cardiovasc. Transl. Res.* **3**, 478–486 (2010).
31. Liu, Z. et al. The influence of chitosan hydrogel on stem cell engraftment, survival and homing in the ischemic myocardial microenvironment. *Biomaterials* **33**, 3093–3106 (2012).
32. Lu, W.-N. et al. Functional improvement of infarcted heart by co-injection of embryonic stem cells with temperature-responsive chitosan hydrogel. *Tissue Eng. Part A* **15**, 1437–47 (2009).
33. Yu, J. et al. The use of human mesenchymal stem cells encapsulated in RGD modified alginate microspheres in the repair of myocardial infarction in the rat. *Biomaterials* **31**, 7012–7020 (2010).
34. Wang, T. et al. Bone marrow stem cells implantation with α-cyclodextrin/MPEG–PCL–MPEG hydrogel improves cardiac function after myocardial infarction. *Acta. Biomater.* **5**, 2939–2944 (2009).
35. Martens, T. P. et al. Percutaneous cell delivery into the heart using hydrogels polymerizing in situ. *Cell Transplant.* **18**, 297–304 (2009).
36. Gaffey, A. C. et al. Injectable shear-thinning hydrogels used to deliver endothelial progenitor cells, enhance cell engraftment, and improve ischemic myocardium. *J. Thorac. Cardiovasc. Surg.* **150**, 1268–1276 (2015).
37. Tokita, Y. et al. Repeated administrations of cardiac progenitor cells are markedly more effective than a single administration: a new paradigm in cell therapy. *Circ. Res.* **119**, 635–651 (2016).
38. Bolli, R. Repeated cell therapy: a paradigm shift whose time has come. *Circ. Res.* **120**, 1072–1074 (2017).
39. Menasche, P. Cardiac cell therapy: lessons from clinical trials. *J. Mol. Cell. Cardiol.* **50**, 258–65 (2011).
40. Malliaras, K. & Marban, E. Cardiac cell therapy: where we've been, where we are, and where we should be headed. *Br. Med. Bull.* **98**, 161–185 (2011).
41. O'Cearbhaill, E. D., Ng, K. S. & Karp, J. M. Emerging medical devices for minimally invasive cell therapy. *Mayo Clin. Proc.* **89**, 259–273 (2014).
42. Koshy, S. T., Ferrante, T. C., Lewin, S. A. & Mooney, D. J. Injectable, porous, and cell-responsive gelatin cryogels. *Biomaterials* **35**, 2477–2487 (2014).
43. Roche, E. T. et al. Comparison of biomaterial delivery vehicles for improving acute retention of stem cells in the infarcted heart. *Biomaterials* **35**, 6850–6858 (2014).
44. Laham, R. J., Hung, D. & Simons, M. Therapeutic myocardial angiogenesis using percutaneous intrapericardial drug delivery. *Clin. Cardiol.* **22**, 6–9 (1999).
45. Ujhelyi, M., Hadsall, K., Euler, D. & Mehra, R. Intrapericardial therapeutics: a pharmacodynamic and pharmacokinetic comparison between pericardial and intravenous procainamide delivery. *J. Cardiovasc Electro.* **13**, 605–611 (2002).
46. Moreno, R., Waxman, S., Rowe, K. & Verrier, R. L. Intrapericardial β-adrenergic blockade with esmolol exerts a potent antitachycardic effect without depressing contractility. *J. Cardiovasc. Pharmacol.* **36**, 722–727 (2000).
47. Hatzistergos, K. E. et al. Bone marrow mesenchymal stem cells stimulate cardiac stem cell proliferation and differentiation. *Circ. Res.* **107**, 913–922 (2010).
48. Zhang, Z. et al. Selective inhibition of inositol hexakisphosphate kinases (IP6Ks) enhances mesenchymal stem cell engraftment and improves therapeutic efficacy for myocardial infarction. *Basic Res. Cardiol.* **109**, 417 (2014).
49. Mathieu, E. et al. Intramyocardial delivery of mesenchymal stem cell-seeded hydrogel preserves cardiac function and attenuates ventricular remodeling after myocardial infarction. *PLoS ONE* **7**, e51991 (2012).
50. Tendera, M. et al. Intracoronary infusion of bone marrow-derived selected CD34+ CXCR4+ cells and non-selected mononuclear cells in patients with acute STEMI and reduced left ventricular ejection fraction: results of randomized, multicentre myocardial Regeneration by Intracoronary Infusion of Selected Population of Stem Cells in Acute Myocardial Infarction (REGENT) trial. *Eur. Heart J.* **30**, 1313–1321 (2009).
51. Assmus, B. et al. Transplantation of progenitor cells and regeneration enhancement in acute myocardial infarction (TOPCARE-AMI). *Circulation* **106**, 3009–3017 (2002).
52. Janssens, S. et al. Autologous bone marrow-derived stem-cell transfer in patients with ST-segment elevation myocardial infarction: double-blind, randomised controlled trial. *Lancet* **367**, 113–121 (2006).
53. Klinker, M. W. & Wei, C.-H. Mesenchymal stem cells in the treatment of inflammatory and autoimmune diseases in experimental animal models. *World J. Stem Cells* **7**, 556–567 (2015).
54. Hodgkinson, C. P., Bareja, A., Gomez, J. A. & Dzau, V. J. Emerging concepts in paracrine mechanisms in regenerative cardiovascular medicine and biology. *Circ. Res.* **118**, 95–107 (2016).
55. Guo, Y. et al. Repeated doses of cardiac mesenchymal cells are therapeutically superior to a single dose in mice with old myocardial infarction. *Basic Res. Cardiol.* **112**, 18 (2017).
56. Pilla, J. J. et al. Early postinfarction ventricular restraint improves borderzone wall thickening dynamics during remodeling. *Ann. Thorac. Surg.* **80**, 2257–2262 (2005).
57. Blom, A. S. et al. Ventricular restraint prevents infarct expansion and improves borderzone function after myocardial infarction: a study using magnetic resonance imaging, three-dimensional surface modeling, and myocardial tagging. *Ann. Thorac. Surg.* **84**, 2004–2010 (2007).
58. Kwon, M. H., Cevasco, M., Schmitto, J. D. & Chen, F. Y. Ventricular restraint therapy for heart failure: a review, summary of state of the art, and future directions. *J. Thorac. Cardiovasc. Surg.* **144**, 771–777 (2012).
59. Naftali-Shani, N. et al. Left ventricular dysfunction switches mesenchymal stromal cells toward an inflammatory phenotype and impairs their reparative properties via Toll-like receptor-4. *Circulation* **135**, 2271–2287 (2017).
60. JDRF. Sernova Corp. announces collaboration with Massachusetts General Hospital to develop novel diabetes treatment with funding support from JDRF (accessed 16 October 2015); go.nature.com/2IEDbB6
61. Makkar, R. R. et al. Intracoronary cardiosphere-derived cells for heart regeneration after myocardial infarction (CADUCEUS): a prospective, randomised phase 1 trial. *Lancet* **379**, 895–904 (2012).
62. Killu, A. M. et al. Trends in percutaneous pericardial access during catheter ablation of ventricular arrhythmias: a single-center experience. *J. Interv. Card. Electrophysiol.* **47**, 109–115 (2016).
63. Maisch, B., Ristić, A. D., Pankuweit, S. & Seferovic, P. Percutaneous therapy in pericardial diseases. *Cardiol. Clin.* **35**, 567–588 (2017).
64. Li, J. et al. Tough adhesives for diverse wet surfaces. *Science* **357**, 378–381 (2017).
65. Cannata, A. et al. Postsurgical intrapericardial adhesions: mechanisms of formation and prevention. *Ann. Thorac. Surg.* **95**, 1818–1826 (2013).
66. Melfi, F. M. A., Menconi, G. F., Chella, A. & Angeletti, C. A. The management of malignant pericardial effusions using permanently implanted devices. *Eur. J. Cardiothorac. Surg.* **21**, 345–347 (2002).
67. Imazio, M. et al. Drainage or pericardiocentesis alone for recurrent nonmalignant, nonbacterial pericardial effusions requiring intervention. *J. Cardiovasc. Med.* **15**, 510–514 (2014).
68. Chaudhry, P. A. et al. Passive epicardial containment prevents ventricular remodeling in heart failure. *Ann. Thorac. Surg.* **70**, 1275–1280 (2000).

Acknowledgements

The authors would like to thank R. Liao, S. Fisch and S. Ngoy from the Brigham and Women's Hospital (BHW) Rodent Cardiovascular Physiology core for their technical support (echocardiographic assessment and rodent surgery) during our 28-day animal studies; R. Padera from BWH for his histological assessment; J. W. Shin and A. Mao

for providing us with luciferase-expressing cells; D. Connolly and the CT scanning core at the Department of Biomedical Engineering, NUI Galway, Ireland; N. Phipps and P. Allen for designing scientific illustrations; Y. Narang, F. Connolly and C. Payne for their technical input; A. Grodzinsky and E. Frank for their generous help and guidance with the diffusion test set-up; and finally T. Ferrante from the Wyss Institute for his imaging expertise. Funding was provided by the Wyss Institute for Biologically Inspired Engineering at Harvard University. E.T.R. was funded by the Institute for Medical Engineering Science at the Massachusetts Institute of Technology, Wellcome Trust/Science Foundation Ireland/Health Research Board Seed Award in Science and a Government of Ireland Postdoctoral Award from the Irish Research Council. W.W and G.P.D. acknowledge support from Science Foundation Ireland under grant SFI/12/RC/2278, Advanced Materials and Bioengineering Research (AMBER) Centre, Royal College of Surgeons in Ireland and Trinity College Dublin, Ireland.

Author contributions

W.W., E.T.R., G.P.D., C.J.W. and D.J.M. designed the study. W.W., E.T.R., C.E.V., K.M., S.I., H.O.N., F.W., R.N.S. and J.C.W. performed the experiments. W.W., E.T.R., N.V.V., B.M., P.E.McH., G.P.D, C.J.W. and D.J.M. analysed and reviewed the data. W.W., E.T.R., G.P.D., C.J.W. and D.J.M. wrote the manuscript. All authors reviewed and edited the manuscript.

Competing interests

Patents describing the device documented in this article have been filed with the US Patent Office. W.W., E.T.R., H.O.N., G.P.D., C.J.W. and D.J.M. are inventors of the following patent application: U.S. 15/557,353. The other authors declare no competing interests.

Additional information

Supplementary information is available for this paper at https://doi.org/10.1038/s41551-018-0247-5.

Reprints and permissions information is available at www.nature.com/reprints.

Correspondence and requests for materials should be addressed to G.P.D. or C.J.W. or D.J.M.

Publisher's note: Springer Nature remains neutral with regard to jurisdictional claims in published maps and institutional affiliations.

nature research

Corresponding author(s): David J. Mooney

☐ Initial submission ☐ Revised version ☒ Final submission

Life Sciences Reporting Summary

Nature Research wishes to improve the reproducibility of the work that we publish. This form is intended for publication with all accepted life science papers and provides structure for consistency and transparency in reporting. Every life science submission will use this form; some list items might not apply to an individual manuscript, but all fields must be completed for clarity.

For further information on the points included in this form, see Reporting Life Sciences Research. For further information on Nature Research policies, including our data availability policy, see Authors & Referees and the Editorial Policy Checklist.

Experimental design

1. Sample size

Describe how sample size was determined.

Bioluminescent-cell-refill study: A pilot study was performed to determine the mean and standard deviation in bioluminescent measurements for both conditions. This data was used to determine an adequate sample size (n=5) for a sufficiently powered study to determine the significance of differences between the pre-refill and post-refill groups.
Functional study: A pilot study was initially performed to determine the treatment effect of Therepi following myocardial infraction. This data was used to inform sample size (n=5) for a sufficiently powered study to detect significant differences between treatment and control groups.

2. Data exclusions

Describe any data exclusions.

The following exclusion criteria were pre-established: cells in the simplified Therepi and in the Therepi systems were assessed for viability in vitro prior to surgery by measuring their bioluminescence with the IVIS spectrum. Devices with bioluminescence less than 109 photons/second were excluded. Male rats and rats below 225 g or above 250 g were excluded. The following rats were also excluded: animals that did not survive the MI surgery, animals where the integrity of the device or the subcutaneous line or port was damaged, animals that did not display blanching of the left ventricle on LAD ligation and animals that had an ejection fraction greater than 60% as assessed by echocardiography at day 0. For the PV data, measurement points that did not form a consistent PV loop due to catheter positioning or other reasons were excluded.

3. Replication

Describe whether the experimental findings were reliably reproduced.

The functional study was not replicated. In vitro studies were reliably reproduced. In vivo studies showing cell refill, and delivery of small molecules, were reliably reproduced.

4. Randomization

Describe how samples/organisms/participants were allocated into experimental groups.

No formal randomization was used but surgeries were carried out on groups, which were alternated. Each group was completed over 2-3 different surgery days.

5. Blinding

Describe whether the investigators were blinded to group allocation during data collection and/or analysis.

No formal blinding was used. Electrocardiography imaging was conducted by an independent operator.

Note: all studies involving animals and/or human research participants must disclose whether blinding and randomization were used.

6. Statistical parameters

For all figures and tables that use statistical methods, confirm that the following items are present in relevant figure legends (or in the Methods section if additional space is needed).

n/a	Confirmed
☐	☒ The exact sample size (*n*) for each experimental group/condition, given as a discrete number and unit of measurement (animals, litters, cultures, etc.)
☐	☒ A description of how samples were collected, noting whether measurements were taken from distinct samples or whether the same sample was measured repeatedly
☐	☒ A statement indicating how many times each experiment was replicated
☐	☒ The statistical test(s) used and whether they are one- or two-sided (note: only common tests should be described solely by name; more complex techniques should be described in the Methods section)
☐	☒ A description of any assumptions or corrections, such as an adjustment for multiple comparisons
☐	☒ The test results (e.g. *P* values) given as exact values whenever possible and with confidence intervals noted
☐	☒ A clear description of statistics including central tendency (e.g. median, mean) and variation (e.g. standard deviation, interquartile range)
☐	☒ Clearly defined error bars

See the web collection on statistics for biologists for further resources and guidance.

Software

Policy information about availability of computer code

7. Software

Describe the software used to analyze the data in this study.

Vevolab (VisualSonics) was used for echocardiography analysis. Labchart 8 was used for PV analysis. Graphpad Prism was used for statistical analysis. Micro-CT 3D reconstructions were performed using CT-Pro (Nikon Metrology), and the surface renderings were generated using VGStudio Max. Images showing penetration of fluorescent albumin across a fibrous capsule were generated in Image J using the Fiji image processing package. Living image software (Perkin Elmer) was used to analyse bioluminescent and fluorescent images generated by the IVIS Spectrum Xenogen 5000. All software are commercially available.

For manuscripts utilizing custom algorithms or software that are central to the paper but not yet described in the published literature, software must be made available to editors and reviewers upon request. We strongly encourage code deposition in a community repository (e.g. GitHub). *Nature Methods* guidance for providing algorithms and software for publication provides further information on this topic.

Materials and reagents

Policy information about availability of materials

8. Materials availability

Indicate whether there are restrictions on availability of unique materials or if these materials are only available for distribution by a for-profit company.

All unique materials are readily available from the authors.

9. Antibodies

Describe the antibodies used and how they were validated for use in the system under study (i.e. assay and species).

No antibodies were used.

10. Eukaryotic cell lines

a. State the source of each eukaryotic cell line used.

For in vitro work proving device concept and in vivo work proving cell refill, clonally derived mesenchymal stem cells from BALB/c mice (D1 ORL UVA [D1] (ATCC® CRL¬12424™) were obtained from American Type Culture Collection (ATCC).
For the 28-day functional study primary mesenchymal stem cells derived from Sprague Dawley rats were purchased from Cyagen (RASMX-01001).

b. Describe the method of cell line authentication used.

ATCC cell lines are subjected to comprehensive and repeated authentication and contamination checks, including short tandem repeat (STR) profiling, cell morphology, karyotyping and cytochrome C oxidase I (COI) testing. Testing was also completed to ensure that cell cultures were free of mycoplasma or other bacterial or fungal agents, conforming to the mycoplasma-testing stipulations recommended by the FDA 'Points to Consider' protocol. The cells also tested negative for bacteria, fungi, and mycoplasma.
Sprague Dawley Mesenchymal stem cells (purchased from cyagen) were assayed for purity using flow-cytometric analysis of cell-surface antigen expression after cryopreservation. Cells are immunofluorescently stained with fluorochrome –conjugated antibodies specific to cell-surface antigens CD29, CD34, CD44, CD45, CD90 and CD11b/c. Cells must show ≥ 70% positivity for expression of cell-surface antigens CD29, CD44 and CD90. Cells must show ≤ 5% positivity for expression of cell-surface antigens CD34, CD45 and CD11b/c. Furthermore, cells were assayed after cryopreservation for their ability of tri-lineage differentiation. Cells must be able to differentiate to osteocytes, adipocytes and chondrocytes when cultured in the appropriate differentiation media.

c. Report whether the cell lines were tested for mycoplasma contamination.

Cells were tested, and absence of mycroplasma contamination was confirmed.

d. If any of the cell lines used are listed in the database of commonly misidentified cell lines maintained by ICLAC, provide a scientific rationale for their use.

No commonly misidentified cell lines were used.

Animals and human research participants

Policy information about studies involving animals; when reporting animal research, follow the ARRIVE guidelines

11. Description of research animals

Provide details on animals and/or animal-derived materials used in the study.

Female Sprague Dawley rats, aged by weight (225-250g), were purchased from Charles River Laboratories.

Policy information about studies involving human research participants

12. Description of human research participants

Describe the covariate-relevant population characteristics of the human research participants.

The study did not involve human research participants.